ELEVENTH EUROPEAN ROTORCRAFT FORUM

Paper No. 34

THE EFFECT OF PITCH RATE ON THE DYNAMIC STALL OF A NACA 23012 AEROFOIL

Lup. Y. Seto

Roderick A.McD. Galbraith

UNIVERSITY OF GLASGOW

September 10-13, 1985

London, England.

THE CITY UNIVERSITY, LONDON, EC1V 0HB, ENGLAND.

THE EFFECT OF PITCH RATE ON THE DYNAMIC STALL OF A NACA 23012 AEROFOIL

LUP. Y. SETO, RODERICK A.McD. GALBRAITH
UNIVERSITY OF GLASGOW

Abstract

The paper presents the results of dynamic stall tests on a NACA 23012 aerofoil when subjected to constant pitch rates about the quarter chord. The tests were performed over a reduced frequency range of $0.00007 < k < 0.04$ and at a corresponding Reynolds and Mach numbers of 1.5×10^6 and 0.11 respectively. The analysis of the data and comparison with other work indicated a possible Mach number dependency of the leading edge suctions influence on stall type and a constancy of the time taken for the stall vortex to develop and pass the trailing edge.

Introduction

For many years, much effort has been expended to gain our current perception of the phenomena associated with dynamic stall of aerofoils (refs. 1, 2, 3). Such understanding is particularly relevant to the development of helicopter rotors, both from a practical and fundamental viewpoint, since the retreating blade is susceptible to dynamic stall as the aircrafts' performance limits are approached. An early and significant experimental study by Ham & Garelick (ref. 4) resulted in a major observation; namely, the formation and subsequent shedding of a vortex from the leading edge of the aerofoil. As this vortex passed rearward over the upper surface, it induced large transients in pressure and hence lift and pitching moment. Later investigations by McCrosky & Fisher (ref. 5) showed that these transient vortex associated rotor loadings were analogous to that oscillatory wing stall. Following the above work, detailed measurements have been made for many aerofoils (ref. 8) and in most cases, under oscillatory pitching motions in nominally 2-dimensional conditions. Other motions and configurations have been tested (refs. 6 & 7) and, in particular, the aerofoil performance when subjected to a constant angular velocity (i.e., ramps).

Complications with oscillatory data are associated with the large data sets required to cover, with reasonable resolution, all the conditions of interest (i.e., variations of amplitude, frequency, mean angle and Mach number (ref. 8)) and the non-linear nature of the model motion. In constrast to this, if one simply considers pitching displacements at constant angular velocity (i.e., ramps), not only are the test cases reduced in number, but increased resolution may be obtained at little extra cost. Further, the sequential timing and manner of the stall, from initiation to completion, may be readily deduced and documented, with evident value to the developers of predictive codes employing a predominantly empirical procedure. The study of such motions, however, does not negate the consideration of oscillatory cases, but if dynamic stall is governed by basic common processes, then it is prudent to include, in fundamental studies, ramp displacements of the type described herein and reported by the present authors (ref. 9).

The present study is, in fact, part of work in progress to investigate the interaction between the trailing edge separation and leading edge conditions and their effect on stall onset. The incentive for this being the susceptibility of some modern rotor sections to significant amounts of trailing edge separation and, further, to provide data for the enhancement of predictive procedures to include reasonable consideration of such separations, (e.g., ref. 10). The clear stated objective provided guidance for the choice of basic aerofoil; a NACA 23012 section (ref. 11). The present paper presents the general gross features of the stall as observed.

Details of the experiments

Using an existing facility at Glasgow (see fig. 1 and refs. 11, 12), a NACA 23012 aerofoil model, with a 0.55m chord, was subjected to constant pitch rate motions ("ramps"), about the quarter chord position up to a maximum deflection of 40°. All the tests were carried out at a Reynolds number of 1.5×10^6 which corresponded to a tunnel speed of 40 m/s. Accordingly, the range of reduced frequencies ($k = \dot{\alpha}c/2V$) was

$$0.00007 \leq k \leq 0.04$$

and, as such, the thirty test conditions (ref. 9) encompass the "quasi-static" type stall, through the changeover to full "dynamic" characteristic stall.

The model was instrumented with thirty miniature pressure transducers located along the chord at the mid-span position, with a maximum upper surface spacing of 7% chord. Their conditioned analogue outputs, and those for wind speed and model displacement, were automatically logged and subsequently processed by a DEC MINC (PDP 11/23), configured to suit the facility (ref. 12). Each transducer output was digitised at a frequency of up to 550 Hz, but this, in general, varied according to pitch rate, such that a maximum of 128 sample sweeps covered the period of model motion. During the data processing, no account was taken of tunnel blockage or interference effects, these being treated as unknown.

These effects were also ignored in the tests for the "static" characteristics, to facilitate direct comparisons with the unsteady case. They are, however, significant as may be seen from fig. 2, where it is shown that the working section dynamic pressure fell by 12% at the point of major stall (separated flow over 65% of the wing chord) and a further 5% at complete stall, after which the aerofoil acted as a bluff body. These data were acquired for both increasing and decreasing angles of attack up to a maximum of 30°. It may be seen that the data are in good agreement and, as such, the dashed line is a simple extrapolation to 40° incidence and this, in conjunction with the static data, defined the maximum reduction in dynamic pressure of the tests performed.

At the maximum pitch rate, however, it may be observed that, at the stall, the dynamic pressure only fell by some 3%. The stall incidence was in the region 34° and this angular displacement took 0.12 seconds. In the remaining 0.36 seconds of the logging sequence,

the dynamic pressure continued to fall and, presumably, would have assumed the equivalent static condition. This then defines the minimum dynamic pressure variation during the test series and so all the data were taken within the shaded area of fig. 2.

The contemporary understanding of dynamic stall development under oscillatory conditions is that, after initiation, a strong vortex builds up on the upper surface close to the leading edge and thence, is convected downstream at a fraction of the free stream velocity (ref. 13). There is thus a finite time for the passage of the vortex over the aerofoil. Obviously, for the ramp tests described herein, if the Reynolds number is held fixed (i.e. constant V) and the reduced frequency increased, a limit will be reached when the stall vortex leaves the trailing edge as the model motion becomes non-linear or has stopped. This condition is illustrated in fig. 3, where both the non-linearity angle and that at which the vortex core is assumed to pass the trailing edge, are plotted as functions of reduced frequency (k); these data cross at $k = 0.023$. Whilst this is a relevant boundary, it is more important to consider the stall onset or initiation, which is dependent on reduced frequency, as dictating the test limit for the effect of pitch rate alone on dynamic stall. It is clear from fig. 3 that the data labelled "stall onset" always occurs within the linear portion of the displacement profile and, hence, the entire data set is valid for a consideration of the effects of pitch rate on stall onset. Also included in this figure is the starting angle necessary to attain the prescribed constant pitch rate.

The most striking feature of fig. 3, as a first estimation, is the linearity of the stall onset data and that of the vortex passing the trailing edge. The significance of this and their relation will be noted later and fully discussed in a future paper.

It is customary, during data reduction, to average several individual cycles or tests, so that the repeatable salient features of the stall process are highlighted, whilst extraneous effects are suppressed. For the current series of tests, the average of five runs was taken. A typical set of unaveraged data is as shown in fig. 4, where it may be seen (fig. 4a) that, for the unstalled condition, i.e., up to 20° incidence, there is a high degree of repeatability. Once the stall has started, however, such repeatability deteriorates, but, although the coefficients may vary markedly in magnitude, their stall developments with respect to incidence are generally in better agreement. Further confirmation of this may be obtained by considering the remaining five illustrations of fig. 4 which show the upper surface pressure development of the five consecutive ramp tests, between which the flow was allowed to settle. It may thus be considered acceptable to highlight the salient features by averaging the data. Once the stall has developed, however, and the foil acts as a bluff body with attendant alternate vortex shedding, the averaging process will be invalidated unless there is in-phase shedding between tests. Data was recorded in this region and, whilst it is of little interest to the present dicussion, the above effect was clearly observed.

Results and Discussion

Figure 5 illustrates the uncorrected "static" characteristics of the NACA 23012 aerofoil as obtained by the above facility. These data were collected for both increasing and decreasing incidence and, hence, the upper surface pressure development (fig. 5b) shows reasonable symetry about the maximum incidence. There is, of course, a delay in re-attaching on the down stroke, but the gross appearance is similar to the upstroke. The important features are, however, that the stall shows the characteristics of very rapid movement of the trailing edge separation over 65% of the chord, at around 14.2° incidence, and an associated reduction in peak suction. This is followed by the fully stalled condition at around 20° incidence with a complete collapse of the leading edge loading.

When the foil was subjected to a constant pitch rate of 3.52 °/s, corresponding to a reduced frequency of 0.0004, little change occured to the characteristic manner of the stall (fig. 6b), although a small amount of "dynamic overshoot" is evident in the aerodynamic coefficients (fig. 6a). The limit to this "Quasi-Static" behaviour occurs at a reduced frequency of 0.004 and a pitch rate of 31 °/s. This case is illustrated in fig. 7 where it may be seen, that, dynamic overshoot of C_M and C_N has occurred, together with a reduction in the lift-curve slope, and there exists the semblence of a vortex produced pressure distribution. The peak section does not, however, completely collapse at the initial stall and has the form of the "quasi-static" case.

Above the transitional value of 0.004, the stall acquires the typical characteristics as depicted in fig. 8. These are, with reference to fig. 8a; a significant reduction in the lift curve slope; large dynamic overshoot of C_N and C_M; C_N build up at the stall with subsequent collapse and associated large negative pitching moment. This build up in C_N (fig. 8b) is normally attributed to a vortex like motion developing on the upper surface, resulting in the observed large suction which then moves down the chord. Of particular interest is both the manner of its initiation and of leaving the trailing edge.

It is observed, that the vortex initiation is associated with a "roll up" in suction in the region of the 20-35% chord location. The presence or absence of this phenomenon, together with the bahaviour of the leading edge suction, may therefore be taken as an indication of the stall type, ie, "quasi-static" or "dynamic". Figure 9, in which the pressure coefficient at the 34% chord position is plotted for various values of reduced frequency, illustrates the change over from "quasi-static" to "dynamic" stall, as occurring in the region of $k = 0.004$. Below this value, the suction increases with increasing incidence and then, at the stall, falls in a manner similar with static behaviour with partial collapse of the leading edge suction as shown in fig. 13. In contrast, for higher values of k, the leading edge suction exhibits a complete collapse at stall (see fig. 13) whereas the suction at 34% chord "rolls up", followed by a collapse and a subsequent repetition from a secondary vortex.

After stall initiation, its progression can be seen from fig. 10

where selected chordal Cp values for the dynamic case (k = 0.02) are presented in the manner of ref 14. These data indicate the stall being initiated towards the leading edge in the region of 30% chord and thence developing towards the leading and trailing edges as shown by the arrows. This type of stall, which is typical of those during the tests (k ≥ 0.004), is comparable with that described by McCroskey (ref. 14), albeit limited trailing edge separation may exist before the Cp roll up at the 34% chord location. Another interesting feature is the small pressure wave travelling up the chord after the vortex has passed or just broken away from the trailing edge. A better illustration of this is given in fig. 11 where the Cp contours show the obvious main dynamic stall vortex progressing down the chord, followed by a suction penetration from the trailing edge. It is thought that this is associated with the breaking away of the main vortex from the trailing edge and a subsequent inrush of fluid over the upper surface into the low pressure region.

From the foregoing it is clear that, over the considered reduced frequency range, three relevant locations for pressure trace considerations are, at the leading and trailing edges and in the vicinity of the 34% chord position. Figure 12 presents these for four relevant reduced frequencies. For all values of k, the first indications of stall occur at the trailing edge with a rise in suction, indicative of trailing edge separation. In the "quasi-static" case (fig. 12a), this separation builds up until there is a rapid forward progression and subsequent fall of both the 34% chord and leading edge suction. The intermediate case (fig. 12b), which is in the region of transition from "quasi-static" to "dynamic", is mixed in that there is an initial small reduction of suction at 34% chord before it rises to what looks like a small vortex, but the full dynamic stall (figs. 12c, 12d) is initiated towards the leading edge (≏ 30% chord) and, although the trailing edge suction increased prior to this, and so indicates that separation has occurred, the dominant effect is that of the vortex like phonomenon moving down the chord and passing the trailing edge into the free stream.

The significance of figs. 12c, 12d is the relative timing of different events. First, apparent trailing edge separation occurs long before the stall vortex initiation and yet, it is around the 30% chord that the dominant stall begins. Second, the stall onset is prior to the leading edge suction collapse for all relevant reduced frequencies. While the effect of trailing edge separation on stall initiation is still unknown, the phasing of events indicates the limited role of the leading edge suction as a stall trigger mechanism. In fact, as figs. 13-15 show, although the manner of leading edge loading changes from partial collapse during "quasi-static" stall to complete collapse during "dynamic" stall, the peak leading edge suction and its associated incidence continue to increase with increasing reduced frequency and are not influenced by the transition from "quasi-static" to "dynamic" stall. One cannot, however, ignore the continual increase in peak velocity and the implied severity of the subsequent adverse pressure gradient which, one might expect, would control separation of the boundary layer close to the leading edge. This should result in a progressive forward movement of the stall onset location when, in fact, it seems to be relatively insensitive to it.

It is now interesting to compare the current finding to that of ref. 15 where it was observed that there was a transfer of stall trigger from trailing edge separation at low pitch rates to leading edge dominance at high pitch rates with a levelling off of both the peak suction and its associated incidence. It must be appreciated that the data presented in ref. 15 were obtained under a test condition of $Re = 2.8 \times 10^6$ and $M = 0.3$, as such local Mach number at the leading edge was in the critical region of $0.85 \rightarrow 1.05$ with strong compressibility effects and a possibility of shock wave development at the leading edge which might have caused the observed level off of peak suction. The difference in the findings thus indicates a possible effect of free stream Mach number on the dominance of the leading edge as a stall mechanism. For low speed tests of current data, which were taken at $Re = 1.5 \times 10^6$ and $M = 0.11$, the maximum local Mach number being around 0.5 even at the highest pitch rate of 335°/s, the stall vortex originated around the 20-35% chord region and was not influenced by the peak suction.

The net results of the above phonomena, are as given in figs. 16 and 18 which show the data relevant to the aerodynamic coefficients C_N and C_M. It is clear from these data that there is considerable uncertainty as to the value of the respective maximum and minimum values, but less so for the angle at which these values occur. Why such scatter is present is unknown but perhaps it is related to the phasing of the dynamic stall vortex build up and the collapse of the leading edge suction; a hypothesis we hope to test. The significantly less scatter associated with the occurance angle of these maximum and minimum values (figs. 17, 19) does encourage the continuation of data averaging for the sampling procedures of the present tests.

It may be observed, however, that for $k \geq 0.004$ (i.e. the "dynamic" case), the maximum value of C_N is always greater than that at the illustrated break point. This suggests that, for the given set up, the stall vortex suction is always sufficiently developed to outweigh the suction lost when that at the leading edge collapses. As mentioned above, the timing of these two events may be crucial in determining the maximum value of C_N which has, during the early vortex development, comparable contributions from the vortex and the leading edge suction. The process is complicated by the vortex having a predominantly mean flow dependency whilst that of the leading edge suction is likely to be associated with the model's motion. The significance of this is, that whenever an aerofoil stalls in the above manner, one must expect much scatter in the data, whilst, if the stall were purely leading edge dominated and initiated immediately behind the peak suction, one might expect a reduction in the evident scatter. Similar arguements are applicable to the pitching moment data, but in this case, the scatter evident in the incidence at which the minimum value occurs is indeed small. The linearity of this and the corresponding pitching moment "break" incidence are qualitatively similar to that of fig. 3 and indicates a mean flow dependency of the process.

This dependency is best illustrated, for the present, by the data of fig. 3 where two significant events of the stall have been chosen, for their high degree of discrimination, to represent the stall onset

and completion. The stall onset was taken as the suction "roll up" at the 34% chord as this gave consistently good resolution when compared to the signals from the 20-30% chordal region. Whilst the latter region may be closer to the stall origin, it was difficult to determine the stall incidence. As such, and since all the upper surface pressure distributions, for the "dynamic" case, were of similar form, the 34% chord location was chosen to indicate that the stall had started. The stall termination was assumed to be at the trailing edge suction peak which gave very good discrimination of that particular event. Whether or not this was the end of the primary stall is of little relevance, because whatever the phonomenon is, it occurs on all the data and is thus a useful timing event. The incidence of these two chosen events was included in fig. 3 and, as mentioned earlier, the linearity of both plots suggests a possible relationship between the two events. In fact, they are co-incident for $k = 0.0$ and so may be represented by

$$\alpha_{TE} = B + m_1 k$$
$$\alpha_0 = B + m_2 k$$

Hence $(\alpha_{TE} - \alpha_0) = k(m_1 - m_2)$,

and since the motion is at constant angular velocity

$$\dot{\alpha}(t_{TE} - t_0) \equiv \dot{\alpha}\Delta T = (\dot{\alpha}c/2v)\,(m_1 - m_2),\ k = \dot{\alpha}c/2v$$

which yields

$$(\Delta TV/C) = (m_1 - m_2)/2 = \text{CONSTANT}$$

This result implies that the normalised time delay between stall onset and completion is a constant, independent of reduced frequency. The stall, once initiated, is therefore mean flow dependent and not governed by the motion of the model. This is a particular result and may be compared with similar work (ref. 13) in which a dependency on k was observed. It is hoped to elaborate on this with work already in progress.

Conclusions

On the basis of the data and discussions presented, additional insight has been gained in the phenomenon of low speed dynamic stall, and the following conclusions are given for the performance of the NACA 23012 aerofoil.

1. There is a reduced frequency ($k = 0.004$) which divides the aerofoils stall phenomena between what may be loosely termed "Quasi-static" and "Dynamic" stall.

2. The distinction between these two types of stall is governed by the characteristic form of the upper surface pressure distribution, in particular the behaviour of the loadings at the leading edge and the 20-35% chord region.

3. Although stalling below a value of $k = 0.004$ is termed Quasi-static, there are dynamic effects.

4. Dynamic stall is initiated in the region of the 20-35% chord.

5. The peak suction collapses after the stall onset and monotonically increases with increased reduced frequency.

6. The scatter in the absolute values of the aerodynamic coefficients is large, but small for the incidence at which they occur.

7. Once initiated, the gross features of the stall vortex are flow dependent and take the same time to develop, independent of reduced frequency.

Acknowledgements

The authors wish to express their thanks to Professor Richards for his support and encouragement. Also, to P. Wilby (RAE Farnborough) and T. Beddoes (Westland Helicopters), for their continued help and discussions. The work was funded by MOD Agreement No. 2048/026 XR/STR, for which the authors were most grateful.

References

1) McCroskey, W.J., The Phenomenon of Dynamic Stall, Lecture Series 1981-84 in Unsteady Airloads and Aeroelastic Problems in Separated and Transonic Flow, von Karman Institute for Fluid Dynamics, 1981.

2) Beddoes, T.S., Short Course in Unsteady Aerodynamics (Rotor Applications), von Karman Institute, 1980.

3) Philippe, J.J., Dynamic Stall: An Example of Strong Interaction between Viscous and Inviscid Flows, AGARD CP-227, 1977.

4) Ham, N.D. and Garelick, M.S., Dynamic Stall Considerations in Helicopter Rotors, AHS J, Vol. 13, No. 2, 1968.

5) McCroskey, W.J. and Fisher, Jr, R.K., Detailed Aerodynamic Measurements on a Model Rotor in the Blade Stall Regime, AHS J, Vol. 17, No. 1, 1972.

6) Beddoes, T.S., Onset of Leading Edge Separation Effects under Dynamic Conditions and Low Mach Number, Paper presented at 34th Annual Forum of AHS, 1978.

7) St. A.O. Hilaire and et al, The Influence of Sweep on the Aerodynamic Loading of an Oscillating NACA 0012 Airfoil, Vol. 1, NACA CR-3092, 1979.

8) McCroskey, W.J. and et al, An Experimental Study of Dynamic Stall on Advanced Airfoil Sections, Vols. 1, 2, 3, NASA TM-84245, 1982.

9) Seto, L.Y. and Galbraith, R.A.McD., The Collected Data for Ramp Function Tests on a NACA 23012 Aerofoil, Vol. 1, Glasgow University Aero. Report 8413, 1984.

10) Beddoes, T.S., Representation of Airfoil Behaviour, Paper 2, AGARD CP-337, 1983.

11) Leishman, J.G., Contributions to the Experimental Investigation and Analysis of Aerofoil Dynamic Stall, Ph.D. Thesis, Glasgow University, 1984.

12) Galbraith, R.A.McD. and Leishman, J.G., A Microcomputer Based Test Facility for the Investigation of Dynamic Stall, Paper E3, International Conference on the Use of the Micro in Fluid Eng., 1983.

13) Carta, F.O., Chordwise Propagation of Dynamic Stall Cells on an Oscillating Airfoil, AIAA 1372 Aerospace Sciences Meeting, paper 75-25, 1975.

14) McCroskey, W.J. and et al, Dynamic Stall on Advanced Airfoil Sections, AHS J, Vol. 26, No. 3, 1981.

15) Wilby, P.G., An Experimental Investigation of the Influence of a Range of Aerofoil Design Features on Dynamic Stall Onset, Paper presented at 10th European Rotorcraft Forum, 1984.

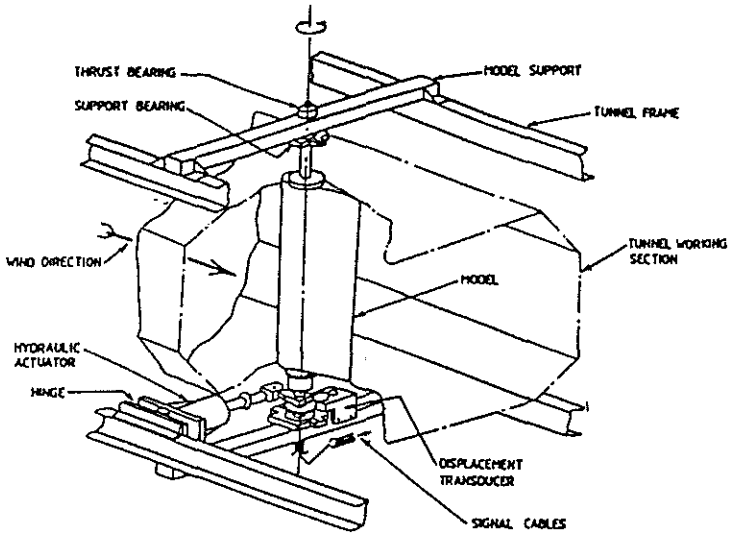

Fig.1 DIAGRAM OF TUNNEL SET UP

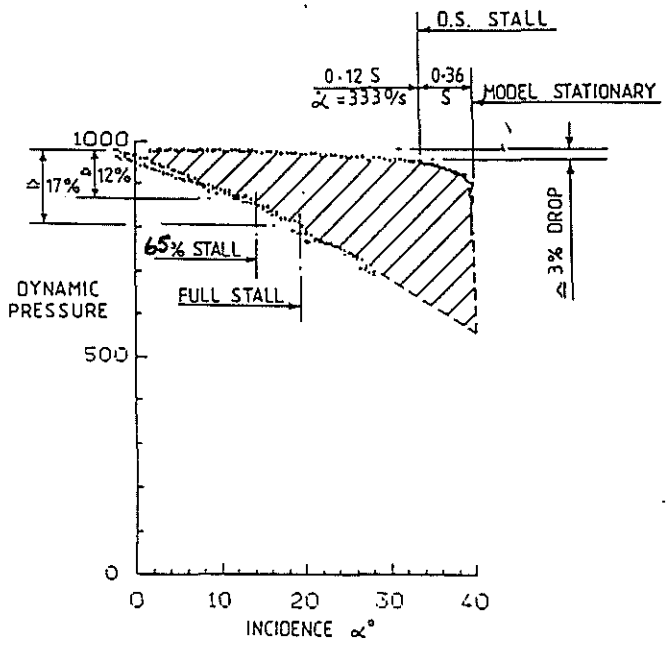

Fig.2. DYNAMIC PRESSURE IN TUNNEL WORKING SECTION

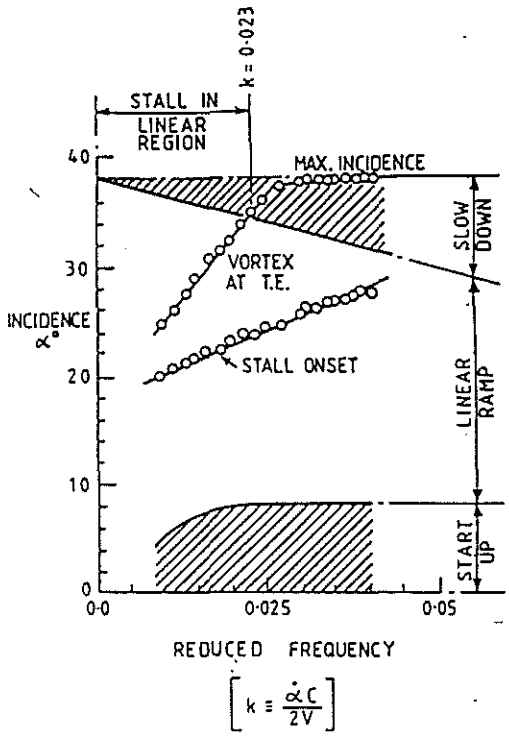

Fig.3. LIMITS TO THE EXPERIMENTS

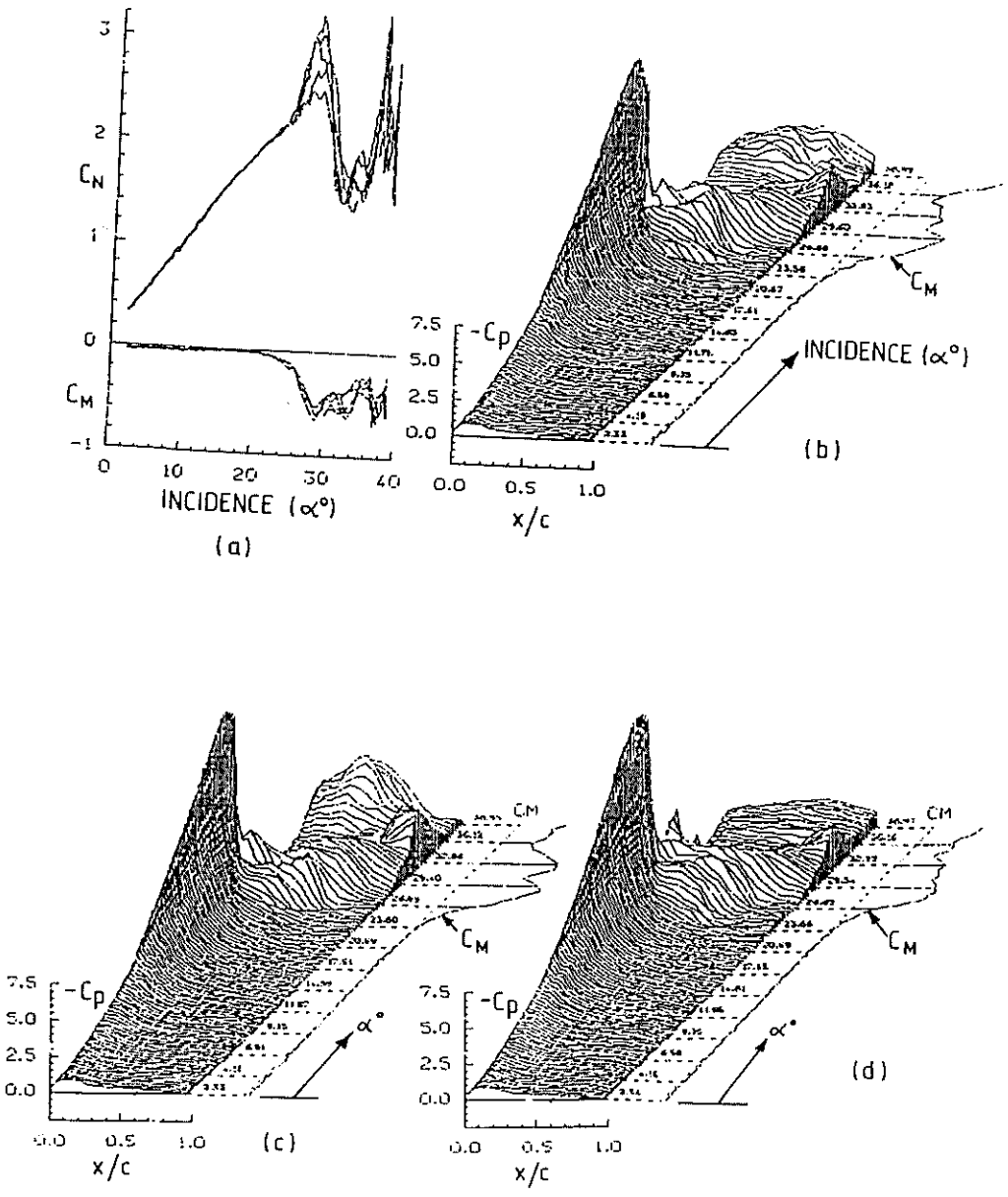

Fig. 4. UNAVERAGED DATA AT k = 0·02.

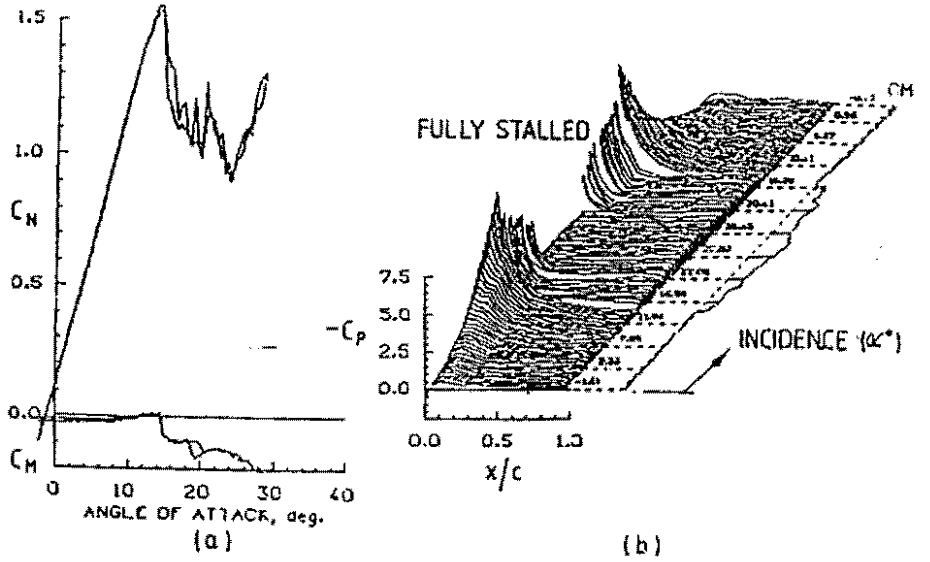

Fig.5 STATIC DATA (k-0·00, $\dot{\alpha}$ = 0°/SEC.)

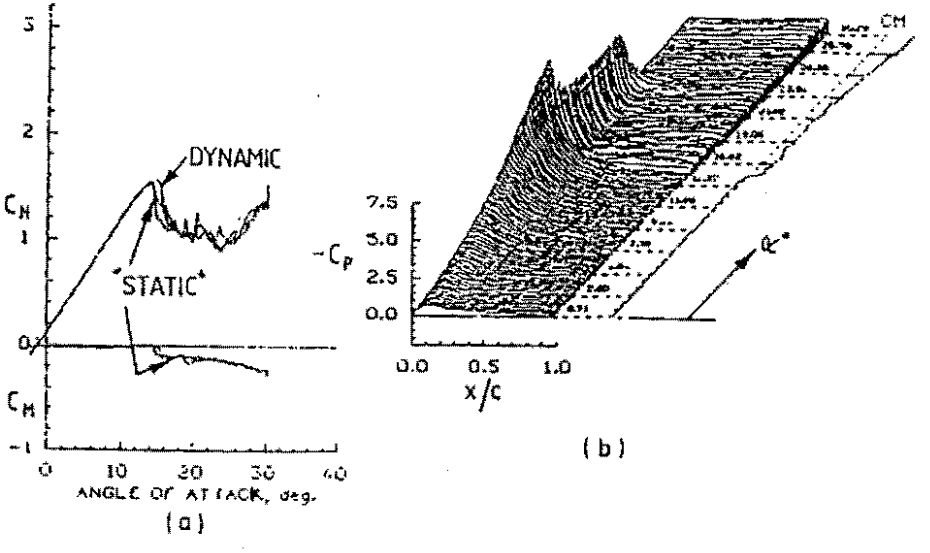

Fig. 6. DYNAMIC DATA (k = 0·0004, 3·52°/SEC.)

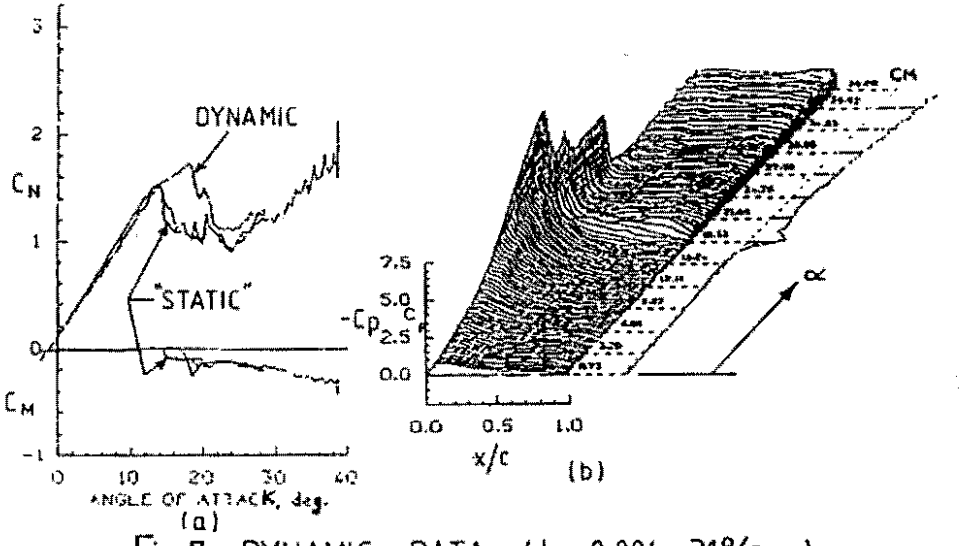

Fig. 7. DYNAMIC DATA (k = 0·004, 31°/sec)

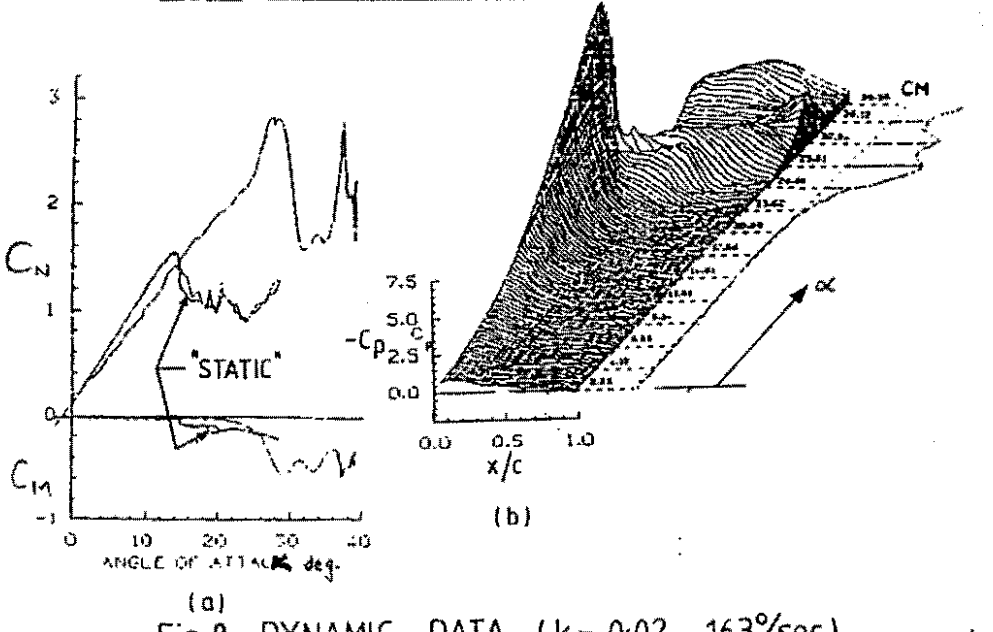

Fig. 8. DYNAMIC DATA (k = 0·02 , 163°/sec)

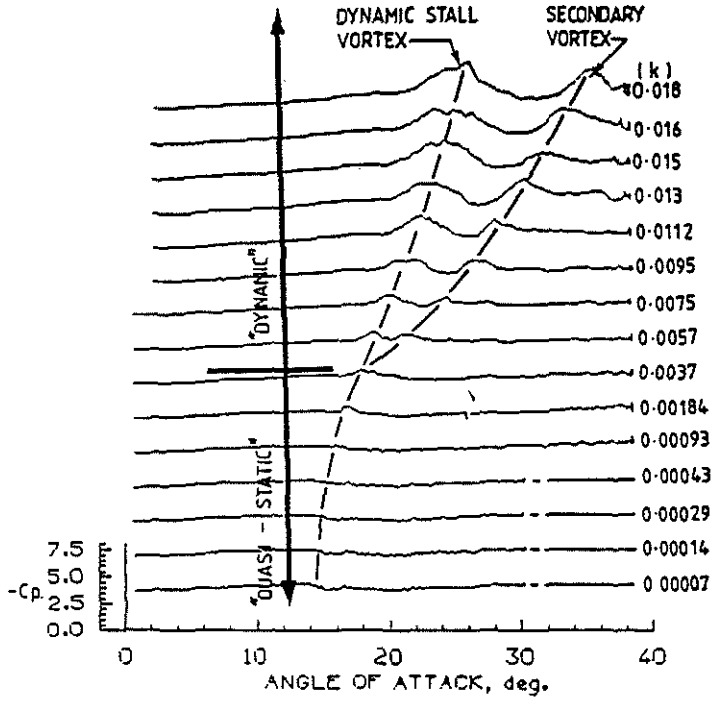

Fig. 9 PRESSURE AT 34% CHORD FOR VARIOUS REDUCED FREQUENCIES.

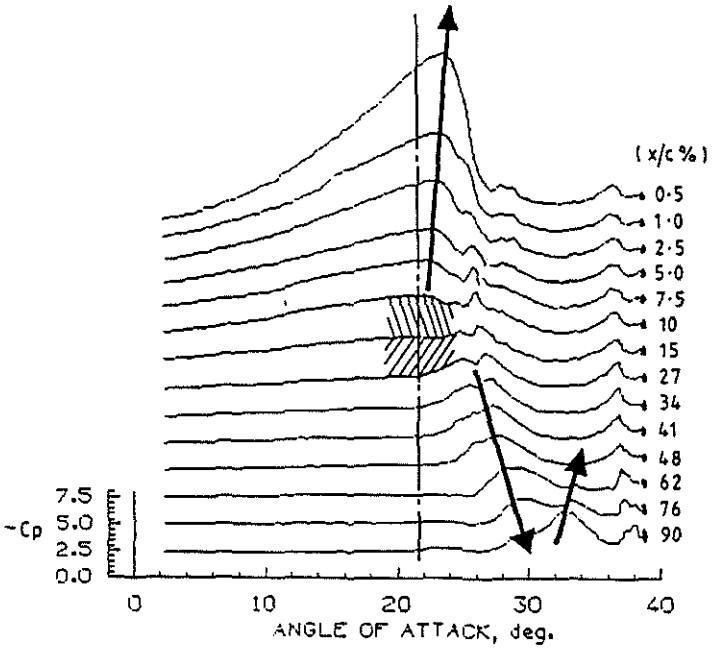

Fig. 10. PRESSURE ON UPPER SURFACE FOR k = 0·02 , $\dot{\alpha}$ = 163°/ SEC.

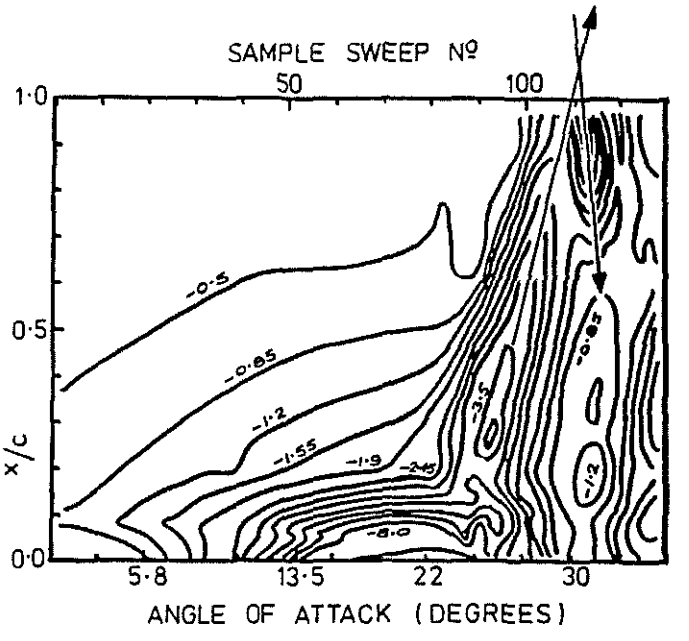

Fig. 11. UPPER SURFACE PRESSURE - COEFFICIENT CONTOURS

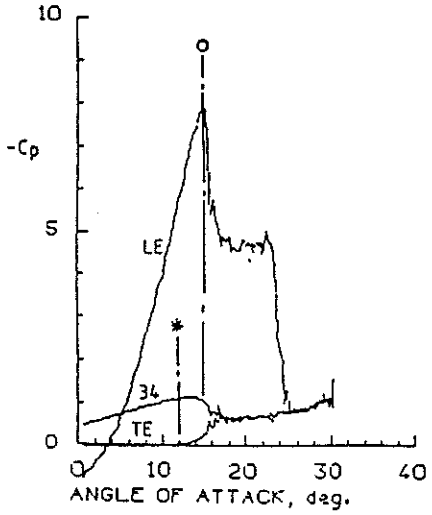

(a) k=0·0004

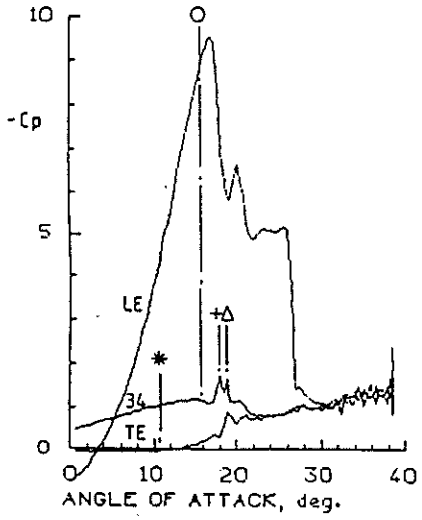

(b) k = 0·004

LE-PRESSURE AT 0·5%C
TE~ " " 97% C
34~ " " 34% C
~T.E. SUCTION RISE
O ~PRESSURE BREAK AT 34%C
+ ~PEAK SUCTION AT 34% C
Δ ~PEAK SUCTION AT T.E.

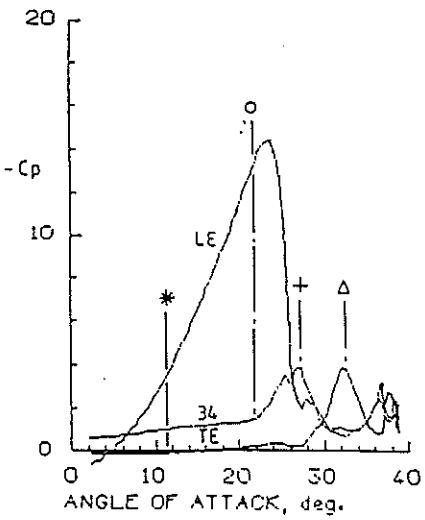

(c) k = 0·02

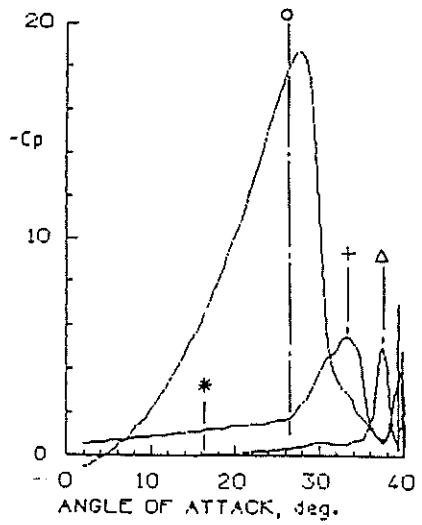

(d) k = 0·04

Fig.12. PRESSURE AT 34%, 0·5% and 97% CHORD FOR VARIOUS REDUCED FREQUENCIES

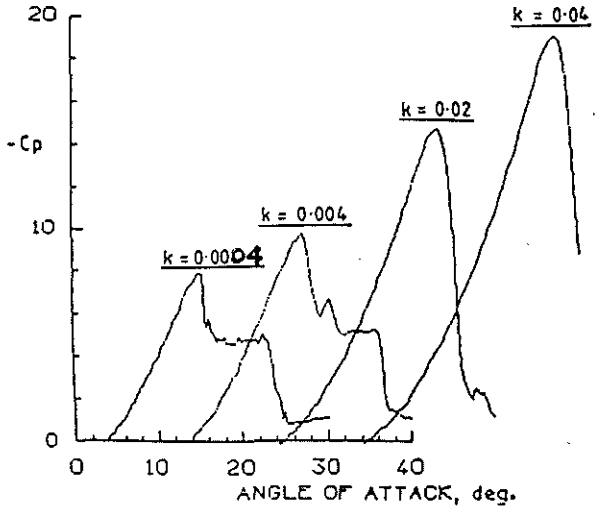

Fig. 13. VARIATION OF Cp AT 0·5% CHORD FOR VARIOUS REDUCED FREQUENCIES

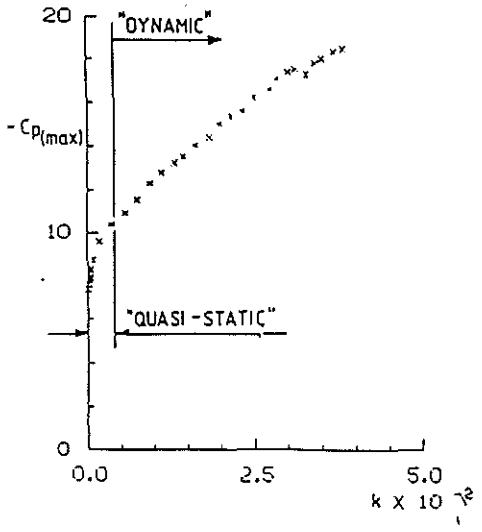

Fig. 14. PEAK SUCTION AGAINST REDUCED FREQUENCY

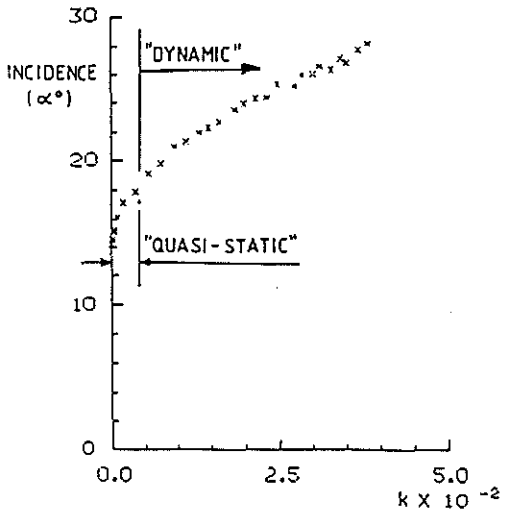

Fig. 15. INCIDENCE AT WHICH PEAK SUCTION OCCURS

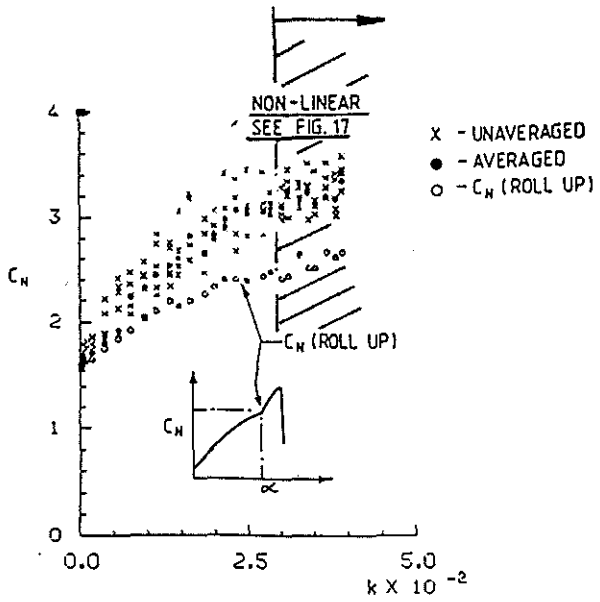

Fig. 16. $C_{N,(max)}$ AND C_N (ROLL UP) AGAINST REDUCED FREQUENCY

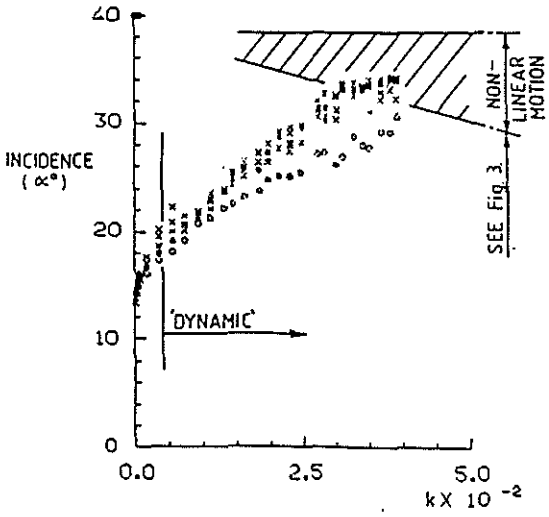

Fig. 17. α ($C_{N\,(MAX.)}$) AND α (C_N ROLL UP) AGAINST REDUCED FREQUENCY.

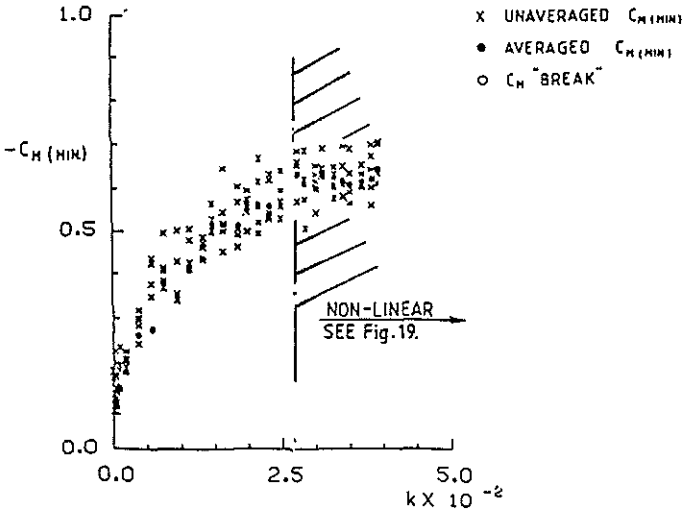

Fig. 18. $C_{M\,(MIN)}$ AGAINST REDUCED FREQUENCY

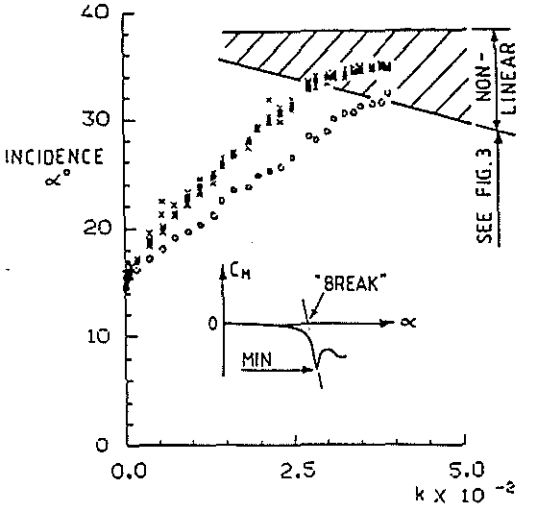

Fig. 19. α (C_{M_MIN}) AND α (C_M BREAK) AGAINST REDUCED FREQUENCY